

High-definition computed tomography for coronary artery stents: image quality and radiation doses for low voltage (100 kVp) and standard voltage (120 kVp) ECG-triggered scanning

Ji Won Lee¹ · Chang Won Kim¹ · Han Cheol Lee² · Ming-Ting Wu³ · Lee Hwangbo¹ · Ki Seok Choo⁴ · June Hong Kim⁵ · Ki-Nam Lee⁶ · Jin You Kim¹ · Yeon Joo Jeong¹

Received: 9 December 2014 / Accepted: 21 May 2015 / Published online: 29 May 2015
© Springer Science+Business Media Dordrecht 2015

Abstract The noninvasive assessment of coronary stents by coronary CT angiography (CCTA) is an attractive method. However, the radiation dose associated with CCTA remains a concern for patients. The purpose of this study is to compare the radiation doses and image qualities of CCTA performed using tube voltages of 100 or 120 kVp for the evaluation of coronary stents. After receiving institutional review board approval, 53 consecutive patients with previously implanted stents (101 stents) underwent 64-slice CCTA. Patients were divided into three different protocol groups, namely, prospective ECG triggering at 100 kVp, prospective ECG triggering at 120 kVp, or retrospective gating at 100 kVp. Two reviewers qualitatively scored the quality of the resulting images for coronary stents and determined levels of artificial lumen narrowing (ALN), stent lumen attenuation increase ratio (SAIR), image noise, and radiation dose parameters. No significant

differences were found between the three protocol groups concerning qualitative image quality or SAIR. Coronary lumen attenuation and in-stent attenuation of 100 kVp prospective CCTA (P-CCTA) were higher than in the 120 kVp P-CCTA protocol (all P s < 0.001). Mean ALN was significantly lower for 100 kVp P-CCTA than for 100 kVp retrospective CCTA (R-CCTA, $P = 0.007$). The mean effective radiation dose was significantly lower ($P < 0.001$) for 100 kVp P-CCTA (3.3 ± 0.4 mSv) than for the other two protocols (100 kVp R-CCTA 6.7 ± 1.0 mSv, 120 kVp P-CCTA 4.6 ± 1.2 mSv). We conclude that the use of 100 kVp P-CCTA can reduce radiation doses for patients while maintaining the imaging quality of 100 kVp R-CCTA and 120 kVp P-CCTA for the evaluation of coronary stents.

Keywords Multidetector computed tomography · Stents · Radiation dosage · Cardiac-gated imaging techniques

✉ Yeon Joo Jeong
lunar9052@hanmail.net

¹ Department of Radiology, Pusan National University Hospital, Pusan National University School of Medicine and Medical Research Institute, #1-10 Ami-Dong, Seo-Gu, Pusan 602-739, Republic of Korea

² Department of Internal Medicine, Pusan National University School of Medicine and Medical Research Institute, #1-10 Ami-Dong, Seo-Gu, Pusan 602-739, Republic of Korea

³ Department of Radiology, Kaohsiung Veterans General Hospital, Kaohsiung, Taiwan, Republic of China

⁴ Department of Radiology, Pusan National University Yangsan Hospital, Yangsan, Korea

⁵ Department of Internal Medicine, Pusan National University Yangsan Hospital, Yangsan, Korea

⁶ Department of Radiology, College of Medicine, Dong-A University, Pusan, Korea

Introduction

Coronary angiography is the clinical gold standard for detecting in-stent restenosis, but it is an invasive procedure that is costly, with associated morbidity and mortality [1]. Therefore, the noninvasive assessment of coronary stents by computed tomography (CT) is an attractive method, because better direct stent lumen visualization is possible by 64-slice CT, which has better spatial and temporal resolutions [2]. Recently, high definition CT (HDCT) scanners with gemstone detectors offering substantially improved in-plane resolution ($0.23 \text{ mm} \times 0.23 \text{ mm}$) were introduced. HDCT can reduce partial volume artifacts due to its higher spatial resolution and better image quality for coronary stent evaluations [3]. However, the radiation dose

associated with coronary CT angiography (CCTA) remains a concern for patients [4, 5].

Previous attempts to reduce CCTA radiation doses have focused on the use of low tube currents, electrocardiogram (ECG)-gated tube current modulation, or prospectively triggered axial acquisition [6]. For ECG-gated tube current modulation, tube currents are reduced according to a specified ECG-gated acquisition window, which is adjusted according to patient heart rate and heart rate stability. In a single-center retrospective study of 64-slice CT [7], the radiation dosage among patients was consequently reduced from 14.8 to 9.4 mSv (36 %). Prospectively gated CCTA has allowed marked reductions in effective radiation doses by about 85 % for patients, while maintaining diagnostic performance at a level comparable to retrospective gated CCTA at low heart rates (up to 70 beats per minute) [8, 9]. Prospectively gated CCTA also has a possible advantage during stent imaging due to reduced cone beam artifacts [10]. The use of low tube voltage is another important approach for dose reduction, because a dose of radiation is proportional to the square of tube voltage in non-obese patients [7, 8]. For the evaluation of stent lumen, however, blooming artifacts are an issue because the lower-energy protons of X-ray beams are more rapidly absorbed, thereby causing beam hardening [2]. At this point, few studies have examined the feasibility of 100 kVp HDCT for the evaluation of coronary stents.

Accordingly, the present study aims to compare image qualities and radiation doses of HDCT performed using tube voltages of 100 or 120 kVp for the evaluation of coronary stents in patients with coronary heart disease.

Materials and methods

Patient population

The study protocol was approved by our Institutional Review Board, and informed consent was obtained from all patients. In this prospective study, 57 consecutive patients that had previously undergone coronary stent implantation were evaluated for regular follow-up between June 2011 and September 2012. Patients were randomly divided by a computer-generated list into three groups by scanning protocol, that is, 100 kVp prospective CCTA (P-CCTA), 100 kVp retrospective CCTA (R-CCTA), or 120 kVp P-CCTA groups.

Patients with a history of previous allergic reactions to iodinated contrast media, impaired renal function (serum creatinine concentration > 1.5 mg/dL), hemodynamic instability, irregular heart rate (atrial fibrillation or frequent premature beats), or an inability to breath-hold were

excluded. We also excluded a patient with a gold-coated stent ($n = 1$) because artifacts are most pronounced for tantalum, gold, or gold-coated stents [11], and patients with significant in-stent restenosis ($n = 3$).

Finally, a total of 101 stents in 53 patients were included in this analysis: 28 stents were scanned by 100 kVp P-CCTA, 39 stents were scanned by 100 kVp R-CCTA, and 34 stents were scanned by 120 kVp P-CCTA.

CCTA acquisition and reconstruction

All examinations were performed using a Discovery 750 HD scanner (GE Healthcare, Milwaukee, WI, USA) at high resolution (0.23 mm isotropic resolution). In the absence of a contraindication, patients with a heart rate (HR) of >65 beats/minute received 50 mg of oral β -blocker (Propranolol hydrochloride) 1 h before examination, and a 0.6 mg sublingual dose of nitroglycerin was administered just prior to examination. We screened patients for contraindications prior to β -blockers administration. CT imaging data were acquired with the holding of patients' breath in deep inspiration to eliminate respiratory motion artifacts. CCTA was performed after determining peak enhancement using a "test bolus" protocol (10 ml of contrast agent [Ultravist 370; Bayer Schering Healthcare, Berlin, Germany] followed by 20 ml of saline solution, both at flow rates of 4 ml/s). Time to peak enhancement was measured by tracking an ellipsoid region of interest in the ascending aorta above the coronary ostia. Sequential scans with an interval time of 1 s were acquired 8 s after starting the contrast injection. Image acquisition was started with a delay corresponding to the measured contrast transit time plus 5 s. We used a triple-phase contrast protocol: 70 ml of contrast agent, followed by 30 mL of 30 % mixed saline (70 % saline and 30 % contrast agent), followed by a 20-mL saline flush.

Scanning parameters included a rotation of 350 ms, 64×0.625 mm collimation, tube voltage 100 or 120 kVp, and a craniocaudal direction. The tube current for 100 kVp P-CCTA was 700 mA, and the tube current for 120 kVp P-CCTA was 600 mA. All scans in the retrospective group were conducted using ECG-gated tube current modulation (peak current 600 mA during 40–80 % of the R–R interval, and a minimal tube current of 120 mA for the remainder of the cycle).

Usually, reconstructions to visualize stent lumens were obtained at 75 % of the RR-cycle using a HD standard reconstruction algorithm with a slice thickness of 0.625 mm. Whenever necessary, however, images were reconstructed at 5 % intervals of the cardiac cycle to enable the assessment of coronary arteries in the cardiac phase with minimal motion.

Assessment of image quality

Image analyses were performed at a dedicated workstation (Advantage Workstation with CardIQ software, version 4.5, GE Healthcare, Milwaukee, WI, USA). Qualitative image analysis was performed by two independent, blinded radiologists (J.W.L and Y.J.J) with 3 and 6 years of CCTA experience, respectively. Axial slices and curved multi-planar reformations were analyzed using a window width of 1200 Hounsfield unit (HU) and window level of 240 HU [12]. Qualitative image qualities of stents were evaluated using a four-point score (Fig. 1), defined as follows: 1 = excellent quality with no artifacts in stent vicinities, 2 = good quality with discrete stent blurring and small streak artifacts emitting shadows on at least one level, 3 = moderate image quality with blurred stent margins and broader streak artifacts extending <4 mm from stent centers, and 4 = poor image quality with inadequate delineation

between stents and surrounding fatty tissues with streak artifacts extending ≥ 5 mm from stent centers. A score of 4 was considered unacceptable for coronary stent image quality assessment [13]. Reasons for non-evaluable stents were evaluated. Stent diameter, type and location were also recorded.

Quantitative image analysis was also performed by the two independent, blinded observers using a window width of 1200 HU and a window level of 240 HU. Patients with non-evaluable stents were excluded in this analysis. Image noise was measured by placing a circular region of interest (ROI) with a diameter of 20 mm in the aortic root, and was defined as its standard deviation (SD). The observers measured attenuation values inside native coronary vessels using the ROI technique (Fig. 2a). Measurements were repeated three times, and the mean values were calculated. In-stent diameters (proximal, middle, distal) were measured using electronic calipers. Attenuation values inside

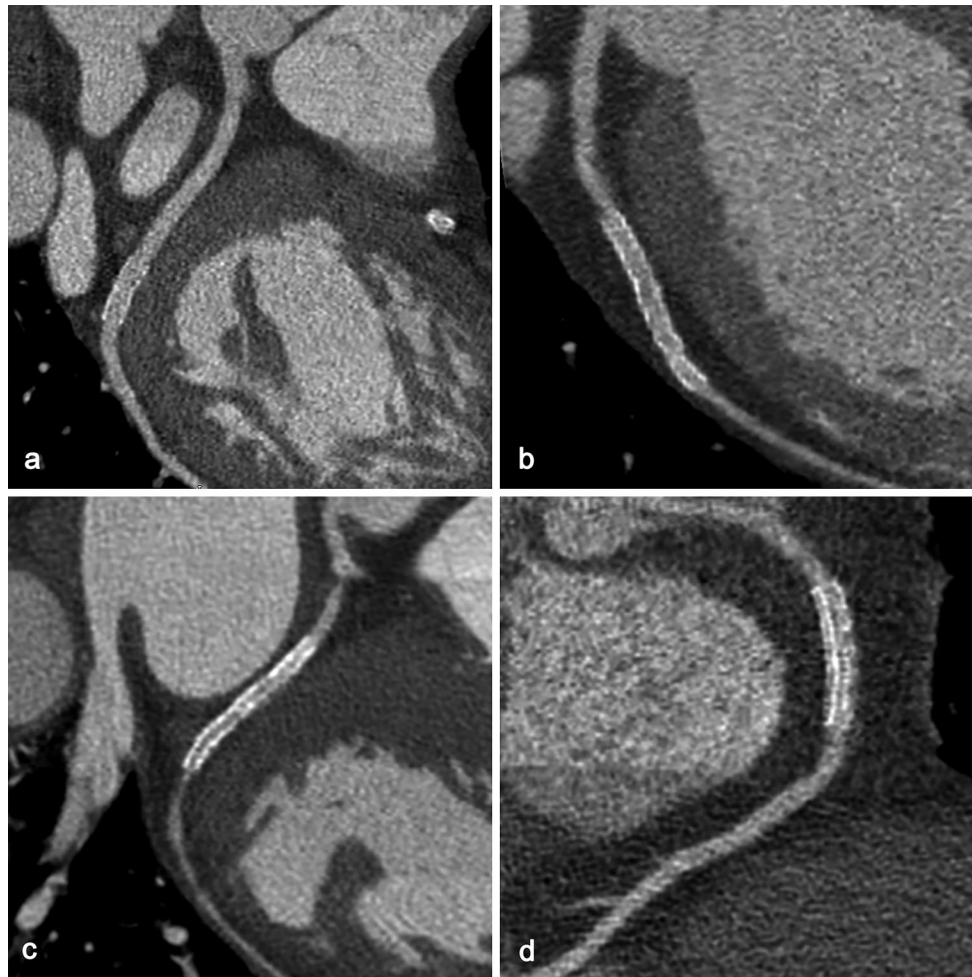


Fig. 1 Image quality assessment using a four-point grading scale. Curved multiplanar reformatted CT images showing excellent image quality with a score of 1 (a), good image quality with a score of 2 (b),

moderate image quality with a score of 3 (c), and poor image quality with a score of 4 (d)

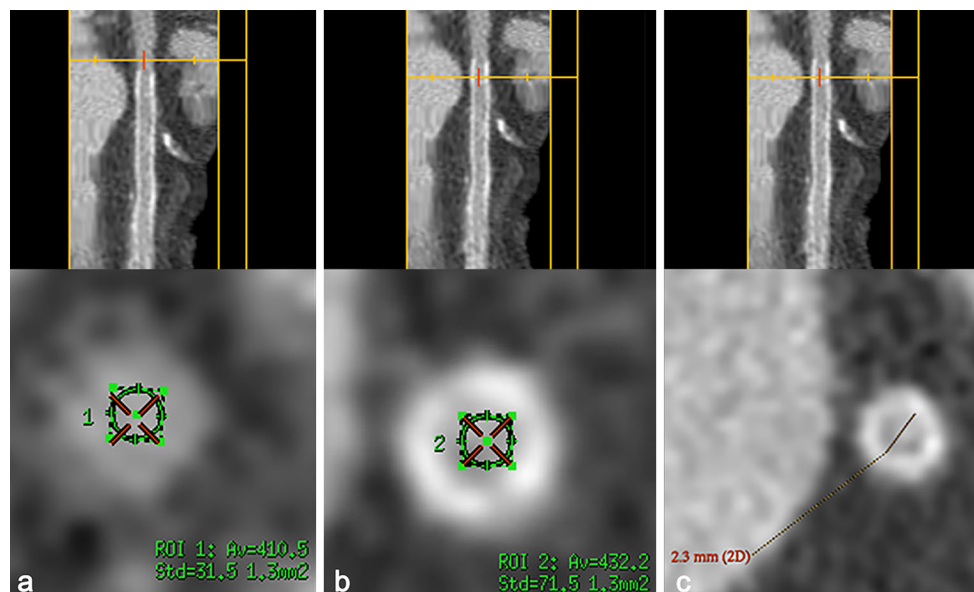


Fig. 2 A 39-year-old man with a coronary stent in the left anterior descending artery. Curved multiplanar reformatted CT images and transverse sections of the coronary artery illustrating the method used to draw a ROI in the native coronary vessel (a) and in the proximal

portion of the coronary stent lumen (b), as well as the method used to measure stent diameters in the proximal portion of coronary stents (c). ROI region of interest

visible stent lumens (proximal, middle, distal) were determined, and mean diameters and values at three different levels were calculated (Fig. 2b, c). These mean diameters and attenuation values were representative of in-stent diameter and attenuation values inside stent lumens. These measurements were performed on the plane perpendicular to the long axis of the vessel using a zoomed field of view. ROIs were drawn as large as possible, while carefully avoiding stent struts and calcifications. To assess the attenuation effects of metallic stent struts on luminal displays, stent lumen attenuation increase ratios (SAIR) were calculated using the following equation: $SAIR = (\text{in-stent attenuation} - \text{coronary lumen attenuation}) / \text{coronary lumen attenuation}$ [14, 15]. A higher value represents the greater blooming effect of metallic stent struts and poorer image quality. To quantify the blooming effects of metallic stent struts, artificial lumen narrowing (ALN) was calculated using the following equation: $ALN = (\text{nominal stent diameter} - \text{measured lumen diameter}) / \text{nominal stent diameter}$ [16]. A higher value represents the greater attenuation effect of metallic stent struts on luminal display and poorer image quality.

Estimation of radiation dose

Values of volume CT dose index ($CTDI_{vol}$) and dose-length product (DLP) were obtained from scan protocols. Effective radiation doses associated with CT examinations were calculated by multiplying the DLP by the chest-

specific conversion coefficient ($k = 0.014 \text{ mSv mGy}^{-1} \text{ cm}^{-1}$) [17].

Statistical analysis

Statistical analyses were performed using PASW (IBM SPSS Statistics 18 for Windows, Chicago, IL, USA). Means and SDs were calculated for all continuous variables and percentages were calculated for all categorical variables. To determine interobserver levels of agreement for qualitative image quality assessments, Kappa statistics were used. Levels of agreement were defined as fair ($\kappa = 0.21\text{--}0.40$), moderate ($\kappa = 0.41\text{--}0.60$), good ($\kappa = 0.61\text{--}0.80$), or excellent ($\kappa = 0.81\text{--}1.00$). To determine interobserver levels of reliability for attenuation measurements, in-stent diameters or image noise levels were evaluated using intra-class correlation coefficients (ICC), where $ICC < 0.4$ represented poor reliability, ICC between 0.4 and 0.75 represented fair-to-good reliability, and $ICC > 0.75$ represented excellent reliability. The Shapiro–Wilk test was used to test for normality. Continuous variables were compared using one-way analysis of variance (ANOVA) with Bonferroni's correction for normally distributed data. The Kruskal–Wallis test with a Mann–Whitney U test used for ordinal data such as qualitative image quality or non-normally distributed data. Categorical variables were compared using Chi squared statistics. Differences between qualitative image qualities by stent diameter or stent location were compared with Mann–Whitney U tests. Differences between quantitative image

qualities by stent diameter or stent location were compared with Student's *t* test. Probability values of <0.05 were considered statistically significant.

Results

Patients

Patient demographics and stent characteristics in the three scanning protocol groups are shown in Tables 1 and 2. Two of 53 patients (4 %) had undergone coronary stents implantation for the management of ischemic cardiomyopathy. Thirty-one of 53 patients (58 %) already treated with oral β -blocker (bisoprolol fumarate 5 mg once daily). And 4 of 53 patients (8 %) with a HR of >65 beats/min received 50 mg of oral β -blocker 1 h before CT examination. In the 53 patients, a total of 101 stents were examined, including stents in the left anterior descending artery (LAD; $n = 52$), the left circumflex artery (LCX; $n = 17$), and the right coronary artery (RCA; $n = 32$). Each stent was considered independently. Twenty-three patients had one stent, 19 patients had two stents, seven patients had three stents, two patients had four stents, one patient had five stents, and one patient had six stents. Three patients had chest pain, and 50 patients had no symptoms. The mean period of time between stent implantation and CT scanning was 24.7 months (range 0–110 months). The three protocol groups were similar in terms of patient gender, age, body mass index (BMI), HR and HR variability, stent location, stent length, stent diameter and stent thickness.

Image quality

Qualitative image quality results are shown in Fig. 3. The interobserver level of agreement for qualitative image

quality was excellent ($\kappa = 0.85$). Qualitative image quality results were similar for the three protocol groups (Kruskal–Wallis test; $P = 0.953$); mean values were 1.8, 1.9, and 1.8, respectively. No significant difference was found between the three protocol groups for the number of non-evaluable stents (Chi squared test; $P = 0.345$). In the 100 kVp P-CCTA group, 96 % (27/28) of stents had acceptable image qualities ≤ 3 . A stent in the RCA, specifically a 3.5-mm Vision stent (Guidant, Santa Clara, CA, USA), was given a score of 4 because of the presence of beam hardening artifacts with motion artifacts. For the 100 kVp R-CCTA protocol group, 90 % (35/39) of stents were acceptable. Two stents in the LCX and two in the RCA had unacceptable image quality due to blooming artifacts for small stents of 2.75 and 2.5 mm ($n = 2$, LCX) or blooming artifacts with motion artifacts ($n = 2$, RCA). For the 120 kVp P-CCTA protocol group, 97 % (33/34) of stents were acceptable. A 3-mm stent in the LAD (Cypher, Cordis, Miami, FL, USA) was given a score of 4 because of beam hardening artifacts.

The quantitative image quality results are shown in Table 3. An excellent level of interobserver reliability was observed between the two readers for the measurement of in-stent attenuation (ICC = 0.98; 95 % confidence interval 0.97–0.99) and coronary lumen attenuation (ICC = 0.91; 95 % confidence interval 0.87–0.94). In-stent attenuation and coronary lumen attenuation in the 100 kVp group were significantly higher than in the 120 kVp group (Kruskal–Wallis test with a Mann–Whitney U test for in-stent attenuation, ANOVA with Bonferroni's correction for coronary lumen attenuation; all P s < 0.001 , Fig. 4a, b). SAIRs were similar for the three protocol groups (Kruskal–Wallis test; $P = 0.980$). Excellent interobserver reliability was obtained between the two readers for in-stent diameter measurements (ICC = 0.99; 95 % confidence interval 0.98–0.99). ALN was significantly lower in the 100 kVp P-CCTA group than in the 100 kVp R-CCTA group

Table 1 Baseline patient characteristics

Clinical data	100 kVp P-CCTA ($n = 17$)	100 kVp R-CCTA ($n = 18$)	120 kVp P-CCTA ($n = 18$)
Gender			
No. of females	6	5	4
No. of males	11	13	14
Age (year) ^a	63.7 \pm 11.2	59.7 \pm 8.7	60.4 \pm 10.0
BMI (kg/m ²) ^a	24.0 \pm 2.5	24.6 \pm 2.6	24.8 \pm 2.4
HR during scan (bpm) ^a	56.2 \pm 6.5	59.8 \pm 9.2	57.2 \pm 5.6
HR variability ^a	5.1 \pm 8.1	2.9 \pm 2.4	3.0 \pm 2.2

bpm beats per minute, *BMI* body mass index, *HR* heart rate, *No.* number, *P-CCTA* prospective ECG-triggered coronary CT angiography, *R-CCTA* retrospective ECG-triggered coronary CT angiography

^a Results are means \pm standard deviations

Table 2 Stent types, lengths, diameters, and strut thicknesses

Stent characteristics	100 kVp P-CCTA (<i>n</i> = 28)	100 kVp R-CCTA (<i>n</i> = 39)	120 kVp P-CCTA (<i>n</i> = 34)	<i>P</i> value
Type [n (%)]				
Biomatrix	1 (3)	0 (0)	0 (0)	
Cypher	3 (11)	0 (0)	2 (6)	
Driver	2 (7)	0 (0)	1 (3)	
Endeavor	7 (25)	15 (38)	3 (9)	
Promus	3 (11)	9 (23)	9 (26)	
Taxus Liberté	9 (32)	9 (23)	15 (44)	
MULTI-LINK vision	1 (4)	1 (3)	2 (6)	
XIENCE V	2 (7)	5 (13)	2 (6)	
Stent location [n (%)]				
LAD	15 (54)	14 (36)	23 (67)	0.075
LCX	5 (18)	7 (18)	5 (15)	
RCA	8 (29)	18 (46)	6 (18)	
Length (mm) ^a	25.70 ± 7.38	25.86 ± 6.33	25.80 ± 7.76	0.941
Diameter (mm) ^a	3.04 ± 0.51	3.00 ± 0.40	3.07 ± 0.50	0.722
Strut thickness (mm) ^a	0.11 ± 0.02	0.10 ± 0.02	0.11 ± 0.03	0.102

LAD left anterior descending artery, LCX left circumflex artery, *N* number, P-CCTA prospective ECG-triggered coronary CT angiography, RCA right coronary artery, R-CCTA retrospective ECG-triggered coronary CT angiography

^a Results are means ± standard deviations

Fig. 3 Qualitative image qualities evaluated using a four-point scoring system for the three scan protocols. Numbers on columns represent patient percentages. Qualitative image quality results were similar for the three protocol groups (Kruskal–Wallis test; *P* = 0.953). P-CCTA prospective ECG-triggered coronary CT angiography, R-CCTA retrospective ECG-triggered coronary CT angiography

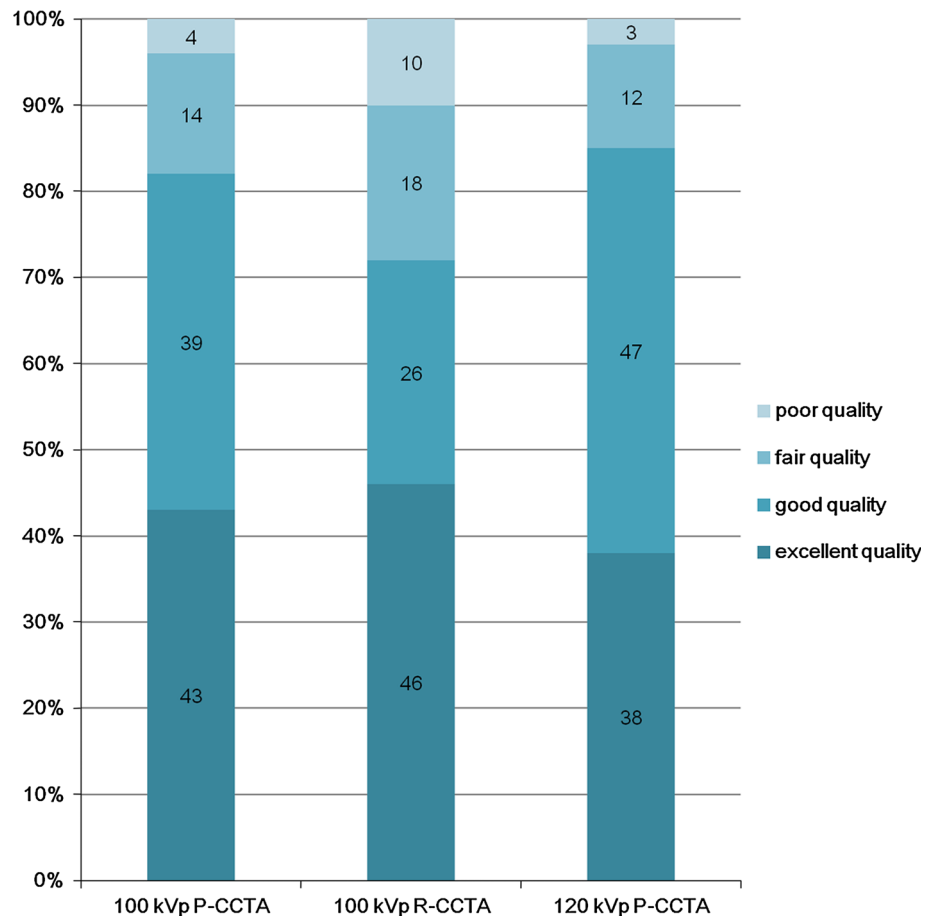


Table 3 Quantitative image qualities in the three study groups

Parameters	100 kVp P-CCTA (<i>n</i> = 27)	100 kVp R-CCTA (<i>n</i> = 35)	120 kVp P-CCTA (<i>n</i> = 33)	<i>P</i> value
Coronary lumen attenuation (HU)	474.1 ± 44.9	470.9 ± 89.5	356.2 ± 57.2	<0.001
In-stent attenuation (HU)	543.3 ± 66.5	549.6 ± 79.3	409.6 ± 57.3	<0.001
SAIR	0.16 ± 0.11	0.19 ± 0.17	0.16 ± 0.12	0.980
ALN	0.29 ± 0.11	0.36 ± 0.10	0.29 ± 0.07	0.004

Results are means ± standard deviations

ALN artificial luminal narrowing, HU Hounsfield unit, P-CCTA prospective ECG-triggered coronary CT angiography, R-CCTA retrospective ECG-triggered coronary CT angiography, SAIR stent lumen attenuation increase ratio

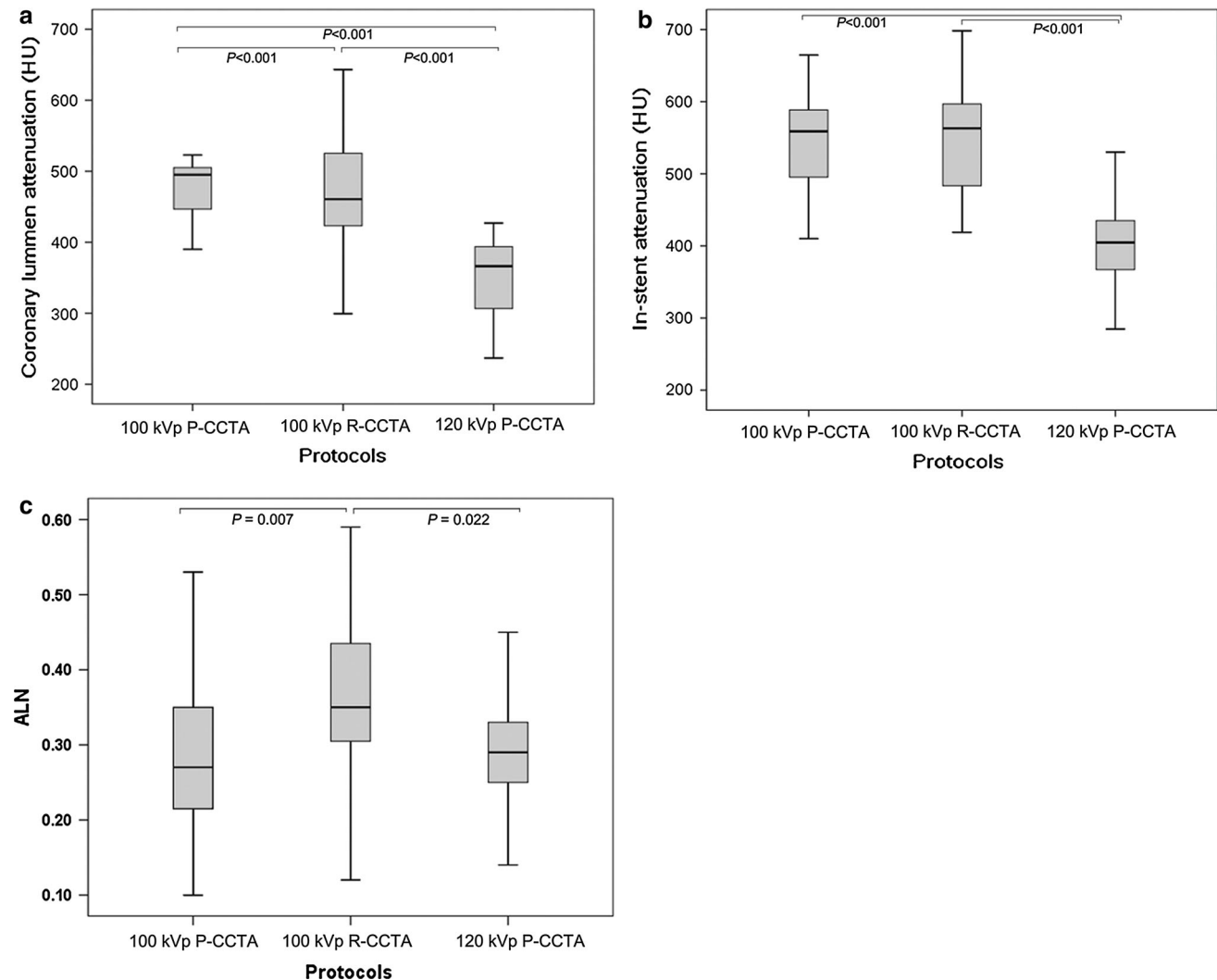


Fig. 4 Quantitative image quality parameters for each scan protocol. **a** Coronary lumen attenuations for 100 kVp protocols were significantly greater than coronary lumen attenuations for the 120 kVp P-CCTA protocol. **b** In-stent attenuations for the 100 kVp protocols were higher than in-stent attenuations for the 120 kVp P-CCTA protocol. **c** ALN for 100 kVp R-CCTA was significantly

higher than ALN for the other two protocols. However, ALN values for 100 kVp P-CCTA and 120 kVp P-CCTA were similar. ALN artificial luminal narrowing, P-CCTA prospective ECG-triggered coronary CT angiography, R-CCTA retrospective ECG-triggered coronary CT angiography

(ANOVA with Bonferroni's correction; $P = 0.007$, Fig. 4c). Excellent interobserver reliability was obtained for the measurement of aortic image noise (ICC = 0.99; 95 % confidence interval 0.99–0.99). Mean values of aortic image noise were 52.8 ± 11.1 HU for the 100 kVp P-CCTA group, 68.8 ± 15.2 HU for the 100 kVp R-CCTA group, and 46.7 ± 9.3 HU for the 120 kVp P-CCTA group. Image noise in the 100 kVp R-CCTA group was significantly greater than in the 100 kVp P-CCTA and 120 kVp P-CCTA groups (Kruskal–Wallis test with a Mann–Whitney U test; all $P_s < 0.001$).

In this study, we included stents with diameters of <3 mm (100 kVp P-CCTA, $n = 11$; 100 kVp R-CCTA, $n = 19$; 120 kVp P-CCTA, $n = 14$). The qualitative image quality results show the mean image quality scores of the stents with diameters of <3 mm were significantly higher than those of the stents with diameters of ≥ 3 mm in the 100 kVp-CCTA groups (Mann–Whitney U tests; 100 kVp P-CCTA: 2.2 ± 0.8 , 1.5 ± 0.8 , $P = 0.021$; 100 kVp R-CCTA: 2.3 ± 1.1 , 1.6 ± 0.9 , $P = 0.030$). However, quantitative image quality results of the stents with diameters of <3 mm were not significantly different than those of the stents with diameters of ≥ 3 mm in the 3 groups (Table 4). ALN of 100 kVp R-CCTA was higher than that of 100 kVp P-CCTA in the subgroup of the stents diameter ≥ 3 mm (one-way ANOVA with Bonferroni's correction; $P = 0.020$). Other qualitative and quantitative image quality results were not significantly

different between the 3 groups in the subgroup of the stents diameter <3 mm and the subgroup of the stents diameter ≥ 3 mm. In this study, we included 48 stents located in the proximal segments (100 kVp P-CCTA, $n = 15$; 100 kVp R-CCTA, $n = 17$; 120 kVp P-CCTA, $n = 16$). Proximal segments include left main coronary artery, proximal LAD, proximal RCA and proximal LCX. Quantitative and qualitative image quality of proximal segments was not significantly different from that of distal segments in each 3 groups (Table 5). Also, Quantitative and qualitative image quality was not significantly different between the 3 groups in the subgroup of proximal or distal segments.

Radiation dose

Values of $CTDI_{vol}$, DLP, and effective doses for each protocol group are presented in Table 6. The effective dose of the 100 kVp P-CCTA group was significantly lower than the effective doses for the other protocol groups (Kruskal–Wallis test with a Mann–Whitney U test; all $P_s < 0.001$). The reduction in voltage from 120 to 100 kVp reduced the effective radiation dose by ~ 28 %. In addition, $CTDI_{vol}$ and DLP values in the 100 kVp P-CCTA group were significantly lower than these values in the other groups (Kruskal–Wallis test with a Mann–Whitney U test; $CTDI_{vol}$ of 100 kVp R-CCTA vs. 120 kVp P-CCTA: 0.005, others all $P_s < 0.001$).

Table 4 Comparison of image quality according to stent diameter in the three groups

	100 kVp P-CCTA	100 kVp R-CCTA	120 kVp P-CCTA
<i>Qualitative image quality</i>			
Stents diameter < 3 mm	2.2 ± 0.8	2.3 ± 1.1	1.9 ± 0.6
Stents diameters ≥ 3 mm	1.5 ± 0.8	1.6 ± 0.9	1.7 ± 0.9
P value ^a	0.021*	0.030*	0.214
<i>Quantitative image quality</i>			
SAIR			
Stents diameter < 3 mm	0.16 ± 0.12	0.18 ± 0.14	0.19 ± 0.17
Stents diameters ≥ 3 mm	0.17 ± 0.11	0.20 ± 0.19	0.16 ± 0.11
P value ^b	0.939	0.747	0.581
ALN			
Stents diameter < 3 mm	0.33 ± 0.14	0.38 ± 0.89	0.31 ± 0.09
Stents diameters ≥ 3 mm	0.26 ± 0.08^c *	0.34 ± 0.11^c *	0.29 ± 0.06
P value ^b	0.259	0.253	0.680

Results are means \pm standard deviations

ALN artificial luminal narrowing, P-CCTA prospective ECG-triggered coronary CT angiography, R-CCTA retrospective ECG-triggered coronary CT angiography, SAIR stent lumen attenuation increase ratio

^a Mann-Whitney U test

^b Student's t test

^c One-way ANOVA with Bonferroni's correction

* $P < 0.05$

Table 5 Comparison of image quality according to stent location in the three groups

Protocol	100 kVp P-CCTA	100 kVp R-CCTA	120 kVp P-CCTA
<i>Qualitative image quality</i>			
Proximal segment	1.9 ± 0.7	2.2 ± 1.2	1.6 ± 0.7
Distal segment	1.7 ± 1.0	1.6 ± 0.9	2.0 ± 0.8
<i>P</i> value ^a	0.440	0.292	0.109
<i>Quantitative image quality</i>			
SAIR			
Proximal segment	0.12 ± 0.10	0.19 ± 0.18	0.15 ± 0.11
Distal segment	0.20 ± 0.11	0.18 ± 0.17	0.19 ± 0.15
<i>P</i> value ^b	0.056	0.837	0.467
ALN			
Proximal segment	0.26 ± 0.11	0.33 ± 0.11	0.28 ± 0.08
Distal segment	0.31 ± 0.10	0.38 ± 0.09	0.32 ± 0.06
<i>P</i> value ^b	0.235	0.163	0.093

Proximal segments include left main coronary artery, proximal left anterior descending artery, left circumflex coronary artery, and right coronary artery. Results are means ± standard deviations

ALN artificial luminal narrowing, P-CCTA prospective ECG-triggered coronary CT angiography, R-CCTA retrospective ECG-triggered coronary CT angiography, SAIR stent lumen attenuation increase ratio

^a Mann–Whitney *U* test

^b Student's *t* test

Table 6 Radiation doses in the three study groups

Parameters	100 kVp P-CCTA (<i>n</i> = 17)	100 kVp R-CCTA (<i>n</i> = 18)	120 kVp P-CCTA (<i>n</i> = 18)	<i>P</i> value
CTDI _{vol} (mGy)	17.3 ± 1.8	29.3 ± 3.0	24.5 ± 5.9	<0.001
DLP (mGycm)	237.6 ± 29.2	476.3 ± 69.3	327.8 ± 87.2	<0.001
Effective dose (mSv)	3.3 ± 0.4	6.7 ± 1.0	4.6 ± 1.2	<0.001

Results are means ± standard deviations

P-CCTA prospective ECG-triggered coronary CT angiography, R-CCTA retrospective ECG-triggered coronary CT angiography

Discussion

The main finding of this study is that HDCT of coronary stents using prospective triggering and 100 kVp significantly reduces the effective radiation dosage with similar image quality measures as 120 kVp P-CCTA imaging. In addition, our results show that 100 kVp R-CCTA did not improve quantitative image quality despite greater radiation exposure over the image qualities of 100 kVp P-CCTA and 120 kVp P-CCTA. No consensus has been reached regarding the optimal tube voltage for coronary stent imaging, although 120 kVp is typically used. However, the present study does show that 100 kVp P-CCTA may be advantageous in terms of lowering the requisite radiation dose for evaluating coronary stents while maintaining qualitative and quantitative image qualities. At this point, no studies have compared the image quality between 100 kVp HDCT and 120 kVp HDCT in the patients with coronary stents.

CCTA imaging of coronary artery stents has evolved as a noninvasive and reliable tool for the diagnostic workup of patients after coronary revascularization therapy. However, the presence of blooming artifacts from stent struts, which are mainly caused by partial volume averaging and beam hardening, limit effective evaluation of stent lumens. In fact, previous studies have reported that stent lumens cannot be assessed in 7.3–42 % of images because of blooming artifacts [12, 18–23]. High tube voltage imaging can be used to mitigate this problem, because higher tube voltages reduce the presence of blooming artifacts by improving beam penetration [2]. However, high radiation exposure among patients increases the risks of severe adverse effects such as carcinogenesis. In the present study, no significant differences were observed between the 100 kVp P-CCTA and 120 kVp P-CCTA groups in terms of SAIR or ALN, the latter of which represents blooming artifacts. The results of the present study are similar to the results of an earlier phantom study conducted with

coronary stents of diameters ≤ 3 mm [24]. In this earlier study, no significant difference was observed between HDCT 100 kVp and 120 kVp datasets in terms of ALN and artificial attenuation [24]. However, Horiguchi et al. [25] reported that 140 kVp P-CCTA provides better coronary in-stent visibility than 120 kVp P-CCTA, 120 kVp R-CCTA, and 140 kVp R-CCTA, even though no significant differences in quantitative image quality (e.g., in ALN and SAIR) were observed between 140 and 120 kVp groups therein [25].

Even though no significant differences were observed between SAIR values or qualitative imaging qualities in the present study, ALN in the 100 kVp P-CCTA group was significantly lower than ALN in the 100 kVp R-CCTA group. The results of the present study correspond to the results of an earlier phantom study that reports that ALN in a prospective axial group was lower than ALN in a retrospective helical group. Furthermore, no significant difference in the increase of artificial attenuation was observed between the two groups [24]. A potential explanation for the reduction of artifacts observed in the prospective group is that additional artifacts occurred in the retrospective helical group due to the helical interpolation and reconstruction process [26].

In addition to lower radiation doses, the use of a lower voltage setting for coronary stent imaging enhances iodine-induced contrast. In the present study, coronary lumen attenuation and in-stent attenuation at 100 kVp P-CCTA were significantly greater (33.7, 32.6 %, respectively) than at 120 kVp P-CCTA. Improvements in attenuation levels are possible using energy levels approximating the K edge of iodine, which occurs at 33.2 keV [27]. The use of a lower kVp protocol means using an energy level that is closer to the optimal energy level for iodine attenuation, and increasing the signal response from vessel-distributed iodine (i.e., from a mean photon energy level of 66 keV at 120 kVp–60 keV at 100 kVp) [27, 28].

In this study, mean image noise for 100 kVp P-CCTA tends to be higher than image noise for 120 kVp P-CCTA without significant difference ($P = 1.0$). Indeed, the imaging noise of CCTA at 100 kVp could be lowered by using adaptive statistical iterative reconstruction (ASIR). A study by Gebhard et al. [12] reports that HDCT using 40 and 60 % ASIR improves intra-stent diameter and area visualization and image quality relative to filtered back projection. However, ASIR was not used in the present study. Thus, further studies on 100 kVp CCTA with ASIR are needed.

Several limitations of the present study require consideration. First, the study was conducted at a single center with a relatively small number of patients, and does not assess the diagnostic accuracy of in-stent restenosis. Although image quality in the 100 kV P-CCTA group is

superior to the image quality in the other groups, the contrast between the coronary artery lumen and the wall may influence the degree of stenotic judgment in patients with in-stent restenosis. Thus, larger-scale, multicenter, prospective studies to evaluate image quality and diagnostic accuracy of 100 kVp P-CCTA for coronary stents are needed. Second, our study has some selection bias. In this study, patients with a gold-coated stent as well as with significant in-stent restenosis were excluded because the visibility of the stent lumen is strongly influenced by stent material and diameter and strut thickness. Third, iterative reconstruction was not used for 100 kVp CCTA, even though this technique is known to improve imaging quality by reducing imaging noise [17]. Because 100 kVp P-CCTA without iterative reconstruction had image qualities similar to 120 kVp CCTA in the present study, 100 kVp P-CCTA with iterative reconstruction may provide superior image quality and reduce noise. Finally, almost all the patients (52/53) included in this study were non-obese Asian patients (BMI range 20.5–31.0 kg/m²). Because image noise increases with body weight, low tube voltage scanning is recommended for non-obese patients (BMI < 30) [29]. Therefore, further research on the image quality of 100 kVp P-CCTA in obese patients would facilitate a more comprehensive understanding.

In conclusion, 100 kVp P-CCTA reduces radiation doses for patients while maintaining image quality in comparison to 100 kVp R-CCTA and 120 kVp P-CCTA for effectively evaluating coronary stents. Therefore, it is conceivable that 100 kVp P-CCTA may be a useful approach for coronary stents evaluation in non-obese patients with nonspecific chest pain.

Acknowledgments This work was supported by the 2013 Clinical Research Grant from Pusan National University Hospital.

Conflict of interest None.

References

1. Pugliese F, Weustink AC, Van Mieghem C, Alberghina F, Otsuka M, Meijboom WB, van Pelt N, Mollet NR, Cademartiri F, Krestin GP, Hunink MG, de Feyter PJ (2008) Dual source coronary computed tomography angiography for detecting in-stent restenosis. *Heart* 94(7):848–854
2. Mahnen AH (2012) CT imaging of coronary stents: past, present, and future. *ISRN Cardiol* 2012:139823
3. Fuchs TA, Stehli J, Fiechter M, Dougoud S, Sah BR, Gebhard C, Bull S, Gaemperli O, Kaufmann PA (2013) First in vivo head-to-head comparison of high-definition versus standard-definition stent imaging with 64-slice computed tomography. *Int J Cardiovasc Imaging* 29(6):1409–1416
4. Hausleiter J, Meyer T, Hermann F, Hadamitzky M, Krebs M, Gerber TC, McCollough C, Martinoff S, Kastrati A, Schomig A, Achenbach S (2009) Estimated radiation dose associated with cardiac CT angiography. *JAMA* 301(5):500–507

5. Halliburton SS, Abbara S, Chen MY, Gentry R, Mahesh M, Raff GL, Shaw LJ, Hausleiter J; Society of Cardiovascular Computed Tomography (2011) SCCT guidelines on radiation dose and dose-optimization strategies in cardiovascular CT. *J Cardiovasc Comput Tomogr* 5(4):198–224
6. Earls JP, Leipsic J (2010) Cardiac computed tomography technology and dose-reduction strategies. *Radiol Clin North Am* 48(4):657–674
7. Hausleiter J, Meyer T, Hadamitzky M, Huber E, Zankl M, Martinoff S, Kastrati A, Schomig A (2006) Radiation dose estimates from cardiac multislice computed tomography in daily practice: impact of different scanning protocols on effective dose estimates. *Circulation* 113(10):1305–1310
8. Qin J, Liu LY, Meng XC, Zhang JS, Dong YX, Fang Y, Shan H (2011) Prospective versus retrospective ECG gating for 320-detector CT of the coronary arteries: comparison of image quality and patient radiation dose. *Clin Imaging* 35(3):193–197
9. Zhao L, Zhang Z, Fan Z, Yang L, Du J (2011) Prospective versus retrospective ECG gating for dual source CT of the coronary stent: comparison of image quality, accuracy, and radiation dose. *Eur J Radiol* 77(3):436–442
10. Hsieh J, Londt J, Vass M, Li J, Tang X, Okerlund D (2006) Step-and-shoot data acquisition and reconstruction for cardiac X-ray computed tomography. *Med Phys* 33(11):4236–4248
11. Mahnken AH, Buecker A, Wildberger JE, Ruebben A, Stanzel S, Vogt F, Gunther RW, Blindt R (2004) Coronary artery stents in multislice computed tomography: in vitro artifact evaluation. *Invest Radiol* 39(1):27–33
12. Gebhard C, Fiechter M, Fuchs TA, Stehli J, Muller E, Stahli BE, Gebhard CE, Ghadri JR, Klaeser B, Gaemperli O, Kaufmann PA (2013) Coronary artery stents: influence of adaptive statistical iterative reconstruction on image quality using 64-HDCT. *Eur Heart J Cardiovasc Imaging* 14(10):969–977
13. Das KM, El-Menyar AA, Salam AM, Singh R, Dabdoob WA, Albinali HA, Al Suwaidi J (2007) Contrast-enhanced 64-section coronary multidetector CT angiography versus conventional coronary angiography for stent assessment. *Radiology* 245(2):424–432
14. Yang WJ, Pan ZL, Zhang H, Pang LF, Guo Y, Chen KM (2011) Evaluation of coronary artery in-stent restenosis with prospectively ECG-triggered axial CT angiography versus retrospective technique: a phantom study. *Radiol Med* 116(2):189–196
15. Ebersberger U, Tricarico F, Schoepf UJ, Blanke P, Spears JR, Rowe GW, Halligan WT, Henzler T, Bamberg F, Leber AW, Hoffmann E, Apfaltrer P (2013) CT evaluation of coronary artery stents with iterative image reconstruction: improvements in image quality and potential for radiation dose reduction. *Eur Radiol* 23(1):125–132
16. Esposito A, Colantoni C, De Cobelli F, Del Vecchio A, Palmisano A, Calandrino R, Del Maschio A (2013) Multidetector computed tomography for coronary stents imaging: high-voltage (140-kVp) prospective ECG-triggered versus standard-voltage (120-kVp) retrospective ECG-gated helical scanning. *J Comput Assist Tomogr* 37(3):395–401
17. Eisentopf J, Achenbach S, Ulzheimer S, Layritz C, Wuest W, May M, Lell M, Ropers D, Klinghammer L, Daniel WG, Pflederer T (2013) Low-dose dual-source CT angiography with iterative reconstruction for coronary artery stent evaluation. *JACC Cardiovasc Imaging* 6(4):458–465
18. Manghat N, Van Lingen R, Hewson P, Syed F, Kakani N, Cox I, Roobottom C, Morgan-Hughes G (2008) Usefulness of 64-detector row computed tomography for evaluation of intracoronary stents in symptomatic patients with suspected in-stent restenosis. *Am J Cardiol* 101(11):1567–1573
19. Krueger KD, Mitra AK, DelCore MG, Hunter WJ 3rd, Agrawal DK (2006) A comparison of stent-induced stenosis in coronary and peripheral arteries. *J Clin Pathol* 59(6):575–579
20. Cademartiri F, Maffei E, Palumbo A, Martini C, Aldrovandi A, Ardissino D, Brambilla V, Coruzzi P, Mollet NR, Krestin GP, de Feyter PJ (2010) CT coronary angiography for the follow-up of coronary stent. *Acta Biomed* 81(2):87–93
21. Rixe J, Achenbach S, Ropers D, Baum U, Kuettner A, Ropers U, Bautz W, Daniel WG, Anders K (2006) Assessment of coronary artery stent restenosis by 64-slice multi-detector computed tomography. *Eur Heart J* 27(21):2567–2572
22. Abdelkarim MJ, Ahmadi N, Gopal A, Hamirani Y, Karlsberg RP, Budoff MJ (2010) Noninvasive quantitative evaluation of coronary artery stent patency using 64-row multidetector computed tomography. *J Cardiovasc Comput Tomogr* 4(1):29–37
23. Gilard M, Cornily JC, Rioufol G, Finet G, Pennec PY, Mansourati J, Blanc JJ, Boschat J (2005) Noninvasive assessment of left main coronary stent patency with 16-slice computed tomography. *Am J Cardiol* 95(1):110–112
24. Yang WJ, Chen KM, Pang LF, Guo Y, Li JY, Zhang H, Pan ZL (2012) High-definition computed tomography for coronary artery stent imaging: a phantom study. *Korean J Radiol* 13(1):20–26
25. Horiguchi J, Fujioka C, Kiguchi M, Yamamoto H, Kitagawa T, Kohno S, Ito K (2009) Prospective ECG-triggered axial CT at 140-kV tube voltage improves coronary in-stent restenosis visibility at a lower radiation dose compared with conventional retrospective ECG-gated helical CT. *Eur Radiol* 19(10):2363–2372
26. Barrett JF, Keat N (2004) Artifacts in CT: recognition and avoidance. *Radiographics* 24(6):1679–1691
27. Huda W, Scalzetti EM, Levin G (2000) Technique factors and image quality as functions of patient weight at abdominal CT. *Radiology* 217(2):430–435
28. Meyer BC, Ribbe C, Kruschewski M, Wolf KJ, Albrecht T (2005) 16-row multidetector CT angiography of the aortiliac system and lower extremity arteries: contrast enhancement and image quality using a standardized examination protocol. *Rof* 177(11):1562–1570
29. Bischoff B, Hein F, Meyer T, Hadamitzky M, Martinoff S, Schomig A, Hausleiter J (2009) Impact of a reduced tube voltage on CT angiography and radiation dose: results of the PROTECTION I study. *JACC Cardiovasc Imaging* 2(8):940–946